Bottomonium Production at $\sqrt{s_{NN}}$ =200 GeV and $\sqrt{s_{NN}}$=5.5 TeV

L. Grandchamp

Lawrence Berkeley National Laboratory, Berkeley, CA 94720

S. Lumpkins

University of Oklahoma, Norman, OK 73019 and

Cyclotron Institute and Physics Department, Texas A&M University, College Station, TX 77843-3366

D. Sun, H. van Hees, and R. Rapp

Cyclotron Institute and Physics Department, Texas A&M University, College Station, TX 77843-3366

(Dated: May 19, 2006)

Properties of bottomonia (Υ, χ_b and Υ') in the Quark-Gluon Plasma (QGP) are investigated by assessing inelastic reaction rates and their interplay with open-bottom states (b quarks or B mesons) and color-screening. The latter leads to vanishing quarkonium-binding energies at sufficiently high temperatures (close to the dissolution point), which, in particular, renders standard gluo-dissociation, $g+\Upsilon \to b+\bar{b}$, inefficient due to a substantial reduction in final-state phase space. This problem is overcome by invoking a "quasifree" destruction mechanism, $g,q,\bar{q}+\Upsilon \to g,q,\bar{q}+b+\bar{b}$, as previously introduced for charmonia. The pertinent reaction rates are implemented into a kinetic theory framework to evaluate the time evolution of bottomonia in heavy-ion reactions at RHIC and LHC within an expanding fireball model. While bottom quarks are assumed to be exclusively produced in primordial nucleon-nucleon collisions, their thermal relaxation times in the QGP, which importantly figure into Υ-formation rates, are estimated according to a recent Fokker-Planck treatment. Predictions for the centrality dependence of Υ production are given for upcoming experiments at RHIC and LHC. At both energies, Υ *suppression* turns out to be the prevalent effect.

PACS numbers: 25.75.Nq 12.38.Mh 25.75.Dw

I. INTRODUCTION

One of the primary objectives of ultrarelativistic heavy-ion collisions is to produce and study the Quark-Gluon Plasma (QGP), a deconfined state of strongly interacting matter which is believed to have existed a few microseconds after the Big Bang. Recent observations from the BNL Relativistic Heavy-Ion Collider (RHIC) indicate that, in a temperature regime $T \simeq$ 1-2 T_c ($T_c \simeq 180$ MeV: (pseudo-) critical temperature [1]), the QGP is not the originally expected weakly interacting gas of quarks and gluons. These observations could, in fact, be related to recent results from lattice Quantum Chromodynamics (lQCD) which suggest the existence of resonance- (or bound-state) like hadronic states up to temperatures of $T \simeq 2T_c$, both in the heavy ($Q\bar{Q}$) [2, 3, 4] and light ($q\bar{q}$) quark sector [1, 5]. For charmonium states this opens the exciting possibility that a substantial part of the final yield arises from (secondary) recombination of c and $\bar{c}$ quarks in the QGP [6, 7] (or at the hadronization transition [8, 9, 10, 11]), as opposed to the originally suggested signature of J/ψ *suppression* [12]. The effectiveness of recombination mechanisms in statistical and kinetic models sensitively resides on a thermal equilibration of the charm- (c-) quark momentum distributions in the QGP [13, 14]. On the one hand, kinetic c-quark equilibrium is not easily conceivable based on perturbative QCD (pQCD) cross sections with thermal light quarks and gluons [15, 16, 17, 18]. On the other hand, a recent study based on resonant rescattering via "D"-meson states in the QGP [17] found substantially smaller c-quark thermalization times (by about a factor of ~ 3 compared to pQCD estimates), being comparable to or even below the expected QGP lifetime at RHIC. Thus, the question arises whether J/ψ suppression, or rather the absence thereof, is an appropriate QGP signature at collider energies. At this point, the prospect of measuring Υ states at RHIC [and the CERN Large-Hadron Collider (LHC)] becomes particularly valuable. Due to their large mass, b quarks are not expected to kinetically equilibrate. Together with their small production-cross sections at RHIC, the situation for bottom appears to be reminiscent to the charm sector at the CERN Super Proton Synchrotron (SPS), in the sense that J/ψ *suppression* has been verified as the dominant effect, with small contributions from regeneration [7, 10].

The main objective of this article is to quantify predictions for bottomonium production at collider energies under simultaneous inclusion of both dissociation and formation reactions. Earlier analyses of bottomonium in heavy-ion reactions have essentially focused on suppression mechanisms, using either the Debye-screening pic-

ture (combined with formation time effects) [19, 20, 21], or gluo-dissociation processes [22, 23], $g+\Upsilon \to b+\bar{b}$ [24]. In the present article we will assess the role of backward reaction channels leading to bottomonium regeneration (secondary production) via $b\bar{b}$ coalescence throughout the QGP phase, as dictated by the principle of detailed balance. Importantly, we incorporate effects of color screening via a substantial reduction of quarkonium binding energies. This, in turn, forces us to replace the gluo-dissociation cross section, which becomes inefficient (and ill-defined) for small binding energies, $\varepsilon_B \lesssim \Lambda_{\rm QCD} \simeq T$, by "quasifree" scattering [10] of thermal partons off the b and $\bar{b}$ quarks in the bottomonium state, $g,q,\bar{q}+\Upsilon \to g,q,\bar{q}+b+\bar{b}$. Despite an apparent suppression by one power of the strong coupling constant, α_S, in-medium reduced binding energies render quasifree dissociation dominant over gluo-absorption due to a much larger phase space [10].

Our article is organized as follows. In Sec. II we give a brief overview of production cross sections for both open and hidden bottom states in hadronic collisions, which will form our baseline for heavy-ion reactions via a scaling by the number of primordial (binary) collisions. In Sec. III we evaluate equilibrium properties of bottomonia in the QGP (complemented by a brief motivation from recent lQCD results in App. A); we compute inelastic cross sections (Sec. III A) and pertinent dissociation rates (Sec. III B) of Υ's and excited states (χ_b and Υ') from scattering off light partons, illustrating limitations of the widely used gluo-dissociation and suitable improvements. In Sec. IV we employ a kinetic-theory framework to study the time evolution of bottomonia in heavy-ion collisions, characterized by an underlying rate equation introduced in Sec. IV A. In addition to inelastic reaction rates, the latter requires further input consisting of (i) a space-time (temperature) evolution of a heavy-ion reaction modeled by a thermal fireball (App. B) and (ii) the equilibrium limit of Υ densities (App. C). Sec. IV B contains our main results for the time evolution of Υ in central Au-Au (Pb-Pb) collisions at RHIC (LHC), with a discussion of the uncertainties related to the Υ equilibrium abundances relegated to appendices D and E. The evolution and feeddown contributions from excited bottomonia are addressed in Sec. IV C. In Sec. V we present our predictions for the centrality dependence of Υ and Υ' production at RHIC and LHC. We summarize and conclude in Sec. VI including an outlook on future improvements of our analysis.

II. INITIAL PRODUCTION OF BOTTOM(ONIUM)

The initial production of $b\bar{b}$ pairs and related fractions of bottomonium states in hard (primordial) nucleon-nucleon (N-N) collisions constitutes an essential input for our subsequent calculations. Throughout the paper we will assume the total number of $b\bar{b}$ pairs in the system to be determined by hard production alone, since, due to the large b-quark mass, $m_b \gg T$, secondary production is expected to be negligible [25] (even under LHC initial conditions as considered below, $m_b/T \gtrsim$ 4-5). The number of $b\bar{b}$ pairs at a given impact parameter, b, of an A-A collision (A=Au and Pb for RHIC and LHC, respectively) can therefore be written as

$$N_{b\bar{b}} = \frac{\sigma_{pp\to b\bar{b}}}{\sigma_{pp}^{\rm inelastic}}\, N_{\rm coll}(b)\, R_y \ , \qquad (1)$$

where $\sigma_{pp}^{\rm inelastic}$ denotes the total inelastic proton-proton cross section ($\simeq$ 42 mb and 78 mb for RHIC and LHC, respectively) [26], and $N_{\rm coll}(b)$ is the number of primordial N-N collisions estimated within the Glauber model. The inclusive cross section, $\sigma_{pp\to b\bar{b}}$, for $b\bar{b}$ production in p-p collisions is taken from recent estimates of Refs. [24, 27]. We use the values $\sigma_{pp\to b\bar{b}} = 2.0$ μb at RHIC ($\sqrt{s_{NN}} = 200$ GeV) and $\sigma_{pp\to b\bar{b}} = 160$ μb at LHC ($\sqrt{s_{NN}} = 5.5$ TeV), which in the latter case includes a factor 0.8 to account for shadowing corrections. Finally, R_y=0.52 (0.29) for RHIC (LHC) denotes the fraction of $b\bar{b}$ pairs within a given rapidity interval ($\Delta y \simeq 3.6$ for two thermal fireballs) which we have estimated from distributions calculated in perturbative QCD [28].

The primordial numbers of bottomonia are not very well known; following Ref. [24, 27], we employ $\sigma_{pp\to\Upsilon}$ =3.5 nb (152 nb) for RHIC (LHC, where we have again included a factor of 0.8 shadowing correction).

The initial number to be used for the thermal evolution has furthermore to account for inelastic processes in the pre-equilibrium stages. We approximate these by the so-called nuclear absorption, which, in principle, can be extracted from data in p-A collisions. Again, this information is rather scarce. We therefore adopt the standard approach employed for charmonia, which consists of a constant (high-energy) nucleon-bottomonium absorption cross section, $\sigma_{\rm nuc}^{\rm abs}$, coupled with a Glauber model for the nuclear overlap function [29]. We note that, at collider energies, coherence effects may induce substantial deviations from the naive collision scaling [30], typically amounting to a significant reduction in absorption. We therefore use rather conservative values for the absorption cross section of $\sigma_{\rm nuc}^{\rm abs} = 3.1$ mb at RHIC (4.6 mb at LHC) [24], which, for simplicity, is assumed to be identical for all bottomonium states.

Different values for $\sigma_{\rm nuc}^{\rm abs}$ will affect the results for the centrality dependence of bottomonium production in A-A collisions presented in Sec. V. On the one hand, the number of "directly" produced bottomonia, defined as the primordial number subjected to suppression only, $N_{\rm dir} = N_{\rm prim}\, S_{\rm nuc}\, S_{\rm QGP}$, depends on the nuclear absorption cross section through the nuclear suppression factor, $S_{\rm nuc}$ (schematically, $S_{\rm nuc} \approx \exp[-\rho_N\, \sigma_{\rm nuc}^{\rm abs}\, L(b)]$ with an effective nuclear density, $\rho_N \simeq$0.14 fm^{-3}, and impact parameter dependent path length, $L(b)$). On the other hand, the number of regenerated bottomonia is practically independent of $\sigma_{\rm nuc}^{\rm abs}$. Thus, whenever the bottomonium yield in an A-A collision at given impact parameter

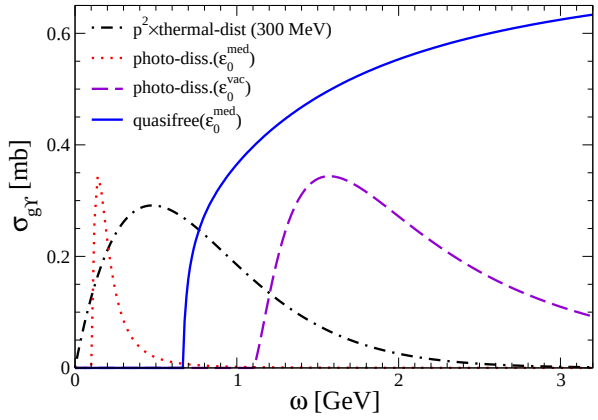

FIG. 1: (Color online) Gluo-dissociation (dashed line: with vacuum binding energy, dotted line: with in-medium reduced binding energy) and quasifree (solid line) cross sections, illustrating the overlap with a thermal gluon distribution at $T = 300$ MeV (dash-dotted line).

is dominated by the direct yield, the percentage error on the nuclear suppression will carry over to the total yield. If the bottomonium yield is dominated by regeneration, the corresponding total will not be sensitive to nuclear absorption.

III. UPSILON PROPERTIES IN THE QGP

In this section we will assess inelastic cross sections and dissociation rates of the Υ and its excited states in the QGP. Our main objective is a combined and consistent treatment of color screening of the heavy-quark potential [12] and inelastic reaction channels. In analogy to the present situation for (ground state) charmonia, and motivated by lQCD results, we assume the bottomonium masses to be constant. The hadronic phase will be neglected altogether throughout this paper. Whenever possible, we will try to motivate necessary assumptions by findings of recent lQCD calculations (see App. A for a brief survey containing more details).

A. Dissociation Cross Sections

The most commonly used process to evaluate the bottomonium (or charmonium) dissociation cross section, $\sigma_Y^{\rm diss}$ (Y=Υ, χ_b, Υ'), on partons is the QCD analogue of photo-dissociation, $g + Y \to b + \bar{b}$ [22, 23]. In Fig. 1, the dashed line represents $\sigma_\Upsilon^{\rm diss}$ for the ground state $\Upsilon(1s)$ with vacuum binding energy, $\varepsilon_B^{\rm vac} \simeq 1.1$ GeV (defined with respect to the $B\bar{B}$ threshold, $2m_B$), as a function of gluon energy ω in the Υ-rest frame. It is peaked around $\omega \simeq 1.5\,\varepsilon_B \simeq 1.5$ GeV, which for moderate plasma temperatures, $T \simeq 300$ MeV, is significantly above average thermal gluon energies, $\omega = 3T$; in other words, the maximum of the cross section has rather little overlap with the phase-space weighted thermal gluon distribution, $p^2 f^g(\omega;T)$ (dash-dotted line in Fig. 1). While an increase in T and a reduction in binding energy (as expected from color screening) initially improves the overlap, a small value of ε_B (toward/close to the dissolution point) eventually leads to a very narrow energy interval where the cross section is active (dotted line in Fig. 1) and thus renders gluo-dissociation increasingly inefficient. Formally this is due to the fact that for a loosely bound (large-size) b-$\bar{b}$ system, the absorption of a hard gluon essentially occurs on a single b quark, in which case energy-momentum conservation cannot be satisfied, and higher orders in the multipole expansion have to be included. This problem is even more severe for the less bound (excited) bottomonia.

To implement effects of color screening we follow the approach suggested in Ref. [10, 31] in the context of charmonia: for small binding energies we approximate Y states as two comoving b and $\bar{b}$ quarks, which individually interact with surrounding thermal partons via lowest-order (quasifree) pQCD scattering [32], $g(q,\bar{q}) + b \to g(q,\bar{q}) + b$ (and likewise for $\bar{b}$). The reaction is considered to lead to Y breakup, $g(q,\bar{q}) + Y \to g(q,\bar{q}) + b + \bar{b}$, if the residual binding energy can be overcome (and conserve overall four momentum). Note that in this approach also thermal (anti-) quarks contribute to bottomonium dissociation via t-channel gluon-exchange. The t-channel singularities are regularized by a gluon Debye-mass, $\mu_D \sim gT$, with $\alpha_S \simeq 0.26$ as fixed in our analysis for charmonia [7] (note that the t-channel gluon-propagator compensates one power in α_S, which formally renders the quasifree cross section of the same order as gluo-dissociation). The result for the quasifree dissociation cross section of $\Upsilon(1s)$ with in-medium binding energy (solid line in Fig. 1) shows a much improved overlap with thermal distributions due to its monotonous rise with gluon energy. The threshold for the result shown is due to a combination of binding energy and thermal parton masses; for massive partons, necessary to reproduce the QGP equation of state, the efficiency of gluo-dissociation is even more suppressed if $\varepsilon_B < m_g \sim gT$. In addition, the quasifree cross section is theoretically better controlled for small values of the binding energy than gluo-dissociation since its main contribution arises from gluons with relatively large (thermal) energies, $\omega \simeq 3T$. Its applicability therefore also encompasses excited bottomonia.

B. Lifetimes

To evaluate bottomonium suppression in the plasma, the inelastic cross section, $\sigma_Y^{\rm diss}$, is converted into a dissociation rate Γ_Y (or inverse lifetime τ_Y^{-1}) by convoluting it with thermal distributions, $f_{g,q}$, of quarks and gluons,

$$\Gamma_Y \equiv \tau_Y^{-1} = \int \frac{d^3k}{(2\pi)^3}\, f_{q,g}(\omega_k,T)\, v_{\rm rel}\, \sigma_Y^{\rm diss}(s)\ . \qquad (2)$$

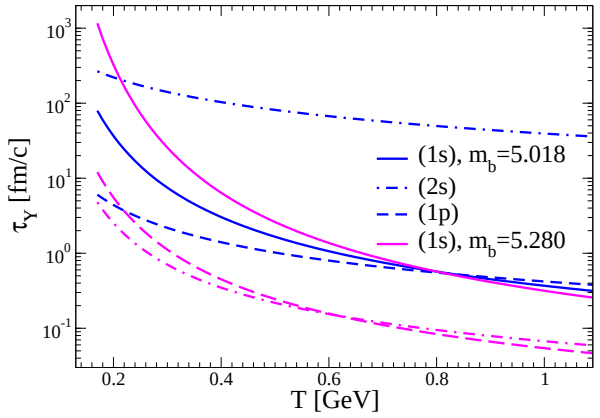

FIG. 2: (Color online) Y lifetimes vs. temperature in a QGP based on the gluo-dissociation process for two (T-independent) values of the bottom-quark mass and pertinent binding energies according to Eq. (7). Solid lines: Υ, dash-dotted lines: Υ', dashed lines: χ_b. The light- (dark-) colored set of curves corresponds to $m_b = 5.280$ GeV ($m_b = 5.018$ GeV).

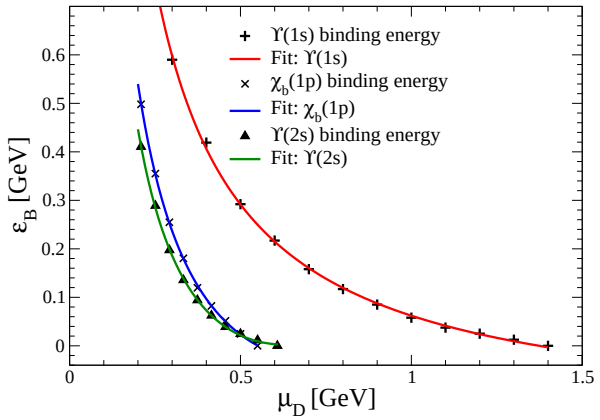

FIG. 3: (Color online) The dependence of Y-binding energies (symbols) on gluon-screening (Debye) mass according to solutions of the Schrödinger equation with a screened Cornell potential [33]. The lines indicate fits used for the numerical implementation in our calculations. The identification with temperature is provided by the perturbative expression for the Debye mass (see text), amounting to, *e.g.*, $\mu_D(T_c) \simeq 325$ MeV.

Here, $s = (q + k)^2$ denotes the total center-of-mass (CM) energy squared of the collision of a Y at rest ($q = (m_Y, \vec{0})$) with a thermal on-shell parton of four-momentum k. We repeat that throughout this paper we use the vacuum masses for the bottomonia (for simplicity we do not distinguish the three spin states of the χ_b but use their average mass).

Let us start by discussing the lifetimes arising from gluo-dissociation using constant (temperature independent) Y binding energies for two different values of the open-bottom threshold ($2m_b$), cf. Fig. 2. For the larger $m_b = 5.280$ GeV (light colored curves), corresponding to the lightest B meson, the lifetimes are rather well-behaved at temperatures relevant for RHIC ($T \lesssim 400$ MeV), *i.e.*, rather large for the Υ (solid line, around 10 fm/c and above, which is significantly longer than the expected QGP lifetime), much smaller for the χ_b (dashed line, 1 fm/c and below), and still slightly smaller for the less bound Υ' (dash-dotted line). However, for temperatures in excess of ∼500 MeV, the Υ' lifetime becomes larger than the one of the χ_b, a first indication of artifacts induced by the gluo-dissociation cross section for small binding energies as discussed in the previous section. This trend becomes more pronounced upon reducing the bottom-quark mass to $m_b = 5.018$ GeV (dark-colored set of lines in Fig. 2), implying $\varepsilon_B^{\Upsilon'} = 13$ MeV and $\varepsilon_B^{\chi_b} = 145$ MeV. In this scenario, the Υ' lifetime is roughly two orders of magnitude larger than the Υ and χ_b lifetimes, which is obviously unrealistic and clearly indicates deficiencies of the gluo-dissociation cross section.

As a more systematic way to include the effects of in-medium heavy-quark potentials in our calculations we make use of the results of Ref. [33] obtained from a Schrödinger equation using a Debye-screened Cornell potential. Assuming a Debye mass of the form suggested by pQCD, $\mu_D = gT$ (with $g \simeq 1.8$ as used in the quasifree cross section), the Υ (χ_b, Υ') binding energy is found to be reduced to about ∼550 MeV (150-200 MeV) at T_c, reaching zero at about 4.3 T_c (∼1.8 T_c), cf. Fig. 3. These values are in reasonable agreement with solutions to a Schrödinger equation based on recent (unquenched) lQCD potentials (except close to T_c) [34]. Since the screening close to T_c might well be less pronounced, our in-medium scenario should be considered as an upper limit of a reduction in binding energies. The pertinent effects in connection with the gluo-dissociation cross section are illustrated by the dark-colored curves in Fig. 4, (the light-colored curves are identical to Fig. 2). Whereas close to T_c the ordering is still reasonable, the strong reduction of ε_B with increasing T rapidly induces a very unrealistic behavior in terms of a reduction in the dissociation rate (increase in lifetime). As discussed above, this artifact is induced by a large decrease in available phase space for the gluo-dissociation cross section which renders bottomonium dissociation a very inefficient reaction as the temperature increases.

As indicated in the previous section the (presumably unphysical) decrease in the reaction rates with increasing T can be remedied by introducing the quasifree dissociation processes which are not limited by phase space and therefore apply to excited states as well. The results are summarized in Fig. 5, where the corresponding Y lifetimes are plotted as a function of temperature. The light-colored lines represent vacuum binding energies with an open-bottom mass of $m_b = 5.280$ GeV. The resulting lifetimes are somewhat larger than the ones using gluo-dissociation (light-colored lines in Fig. 2), but exhibit the (from the size and binding energies) expected hierarchy, $\tau_{\Upsilon'} < \tau_{\chi_b} < \tau_{\Upsilon}$, at all temperatures. The real

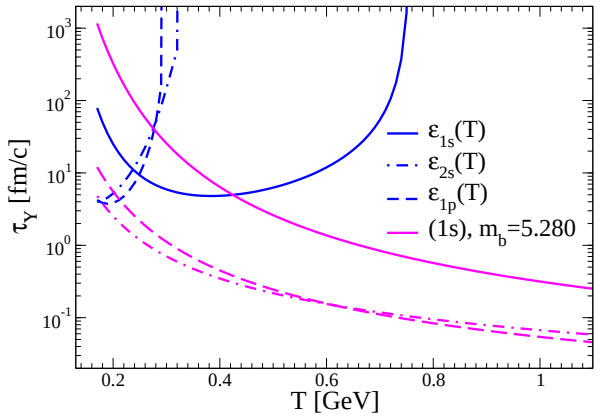

FIG. 4: (Color online) Y lifetimes vs. temperature in a QGP based on gluo-dissociation with an in-medium bottom-quark mass according to in-medium reduced binding energies as computed in Ref. [33] (dark-colored curves). Solid lines: Υ, dash-dotted lines: Υ', dashed lines: χ_b. The light colored curves are identical to Fig. 2, *i.e.*, for constant binding energy with $m_b = 5.280$ GeV.

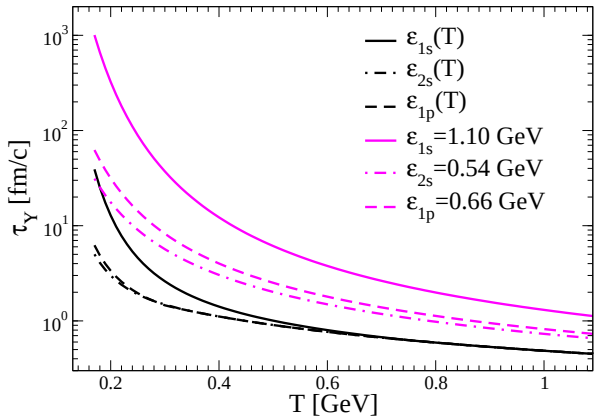

FIG. 5: (Color online) Y lifetimes computed from quasifree dissociation using constant (light set of curves) and in-medium (dark set of curves) binding energies for the Υ (solid line), Υ' (dash-dotted line) and the χ_b (dashed line).

virtue of the quasifree approach manifests itself in a (presumably more realistic) calculation using in-medium (T-dependent) binding energies corresponding to the dark-colored lines. Here, smaller ε_B facilitate bottomonium breakup, and the respective dissociation rates are always larger than the ones using the vacuum values for ε_B. In comparison to the gluo-dissociation results, two further remarks are in order: (i) At the highest temperatures the Y lifetimes are larger than the ones calculated with gluo-dissociation using vacuum binding energies. The main reason for this is that the strong coupling constant, α_S, inherent in the b-$\bar{b}$ Cornell potential necessary to reproduce bottomonium spectroscopy (which also enters the dissociation cross sections), is substantially larger ($\sim$0.5) than in the quasifree calculation ($\sim$0.26). After all, it is the Debye-screening of the potential which is related to an effectively reduced α_S in the medium. (ii) At temperatures $T \lesssim 300(200)$ MeV the gluo-dissociation rates for Υ (Υ', χ_b) using in-medium binding energies are not much smaller than the ones obtained with quasifree destruction. Therefore, both contributions to the rate should, in principle, be accounted for (at higher T, gluo-dissociation with in-medium ε_B is negligible). However, since we have fixed α_S in the charmonium sector using the quasifree process alone to reproduce J/ψ data in Pb-Pb collisions at the SPS, we will refrain from adding the two contributions. In addition, as we will see below, most of the bottomonium suppression at RHIC and LHC occurs at temperatures above $\sim$250 MeV.

Unless otherwise specified, in the following we will use the bottomonium lifetimes pertaining to the quasifree mechanism with in-medium binding energies as our default scenario (we recall that this should provide an upper estimate of the screening effects). For comparison purposes with existing literature, we will also discuss results using the gluo-dissociation reaction alone with vacuum binding energies.

IV. KINETIC THEORY APPROACH

To calculate the time evolution and final abundances of bottomonia in a high-energy heavy-ion collision, we employ a kinetic rate-equation approach, as has recently been applied to charmonium production [6, 7]. On the one hand, such an approach has the appealing feature that it makes explicit contact to equilibrium properties of quarkonia [7], as discussed in the previous section. On the other hand, it does not provide an accurate treatment for processes occurring far from equilibrium, in which case explicit transport calculations are preferable [35, 36].

A. Rate Equation

In the limit that bottom quarks (and/or hadronic open-bottom states which might survive up to $T \simeq 2T_c$ or so) are in thermal equilibrium with the bulk of the system (light partons), the time dependence of the Y number, N_Y, obeys a simplified rate equation given by [37]

$$\frac{\mathrm{d}N_Y}{\mathrm{d}\tau} = -\Gamma_Y \, (N_Y - N_Y^{\mathrm{eq}}) \, , \qquad (3)$$

where spatial (temperature) gradients have been neglected. Here, Γ_Y denotes the Y-dissociation rate discussed in Sec. III B above and N_Y^{eq} the equilibrium number. The first term on the right-hand side of Eq. (3) describes the loss of bottomonia due to dissociation, whereas the second term takes into account regeneration according to the principle of detailed balance,

$$X_1 + Y \leftrightarrow X_2 + b + \bar{b} \, , \qquad (4)$$

where X_1 and X_2 are light-quark or gluon states. Obviously, the backward channel amounts to a recombination

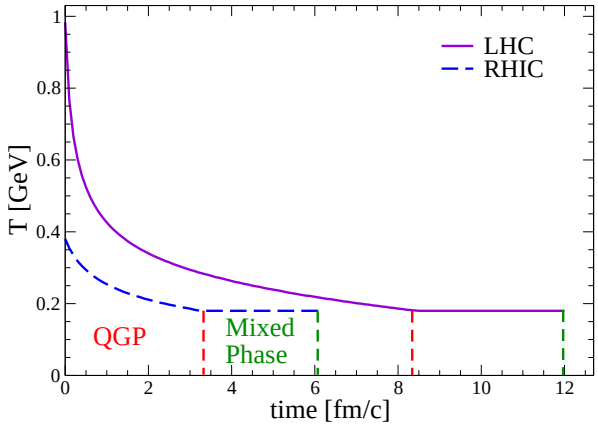

FIG. 6: (Color online) Time evolution of the temperature within our expanding-fireball model for a massive parton gas in central A-A collisions at RHIC (dashed line) and LHC (solid line). The use of massless partons (with $N_f = 2.5$) affects the evolution rather moderately.

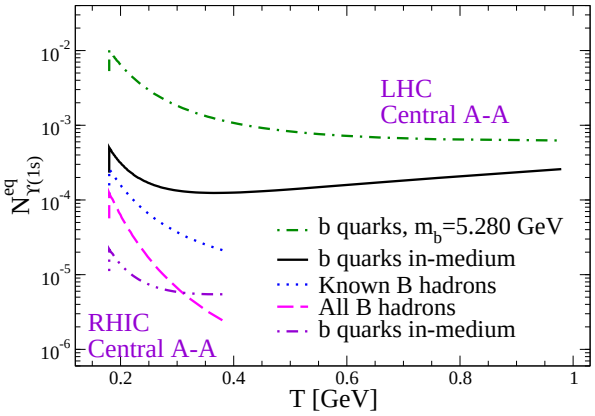

FIG. 7: (Color online) $\Upsilon(1s)$-equilibrium abundances for central A-A collisions at RHIC (lower 3 curves) and LHC (upper 2 curves), according to different scenarios for open-bottom states in the QGP (see text and App. C 1).

(or coalescence) of a b and $\bar{b}$ quark within the QGP. From Eq. (3) it is clear that the regeneration contribution to the Y yield is negligible if either the equilibrium number is small compared to the actual number, $N_Y^{\rm eq} \ll N_Y$ at all times, or the dissociation/recombination processes shut off altogether, *i.e.*, the reaction rate Γ_Υ is very small.

Eq. (3) is amenable to an explicit solution which reads

$$N_Y(t) = S_{\rm QGP}(t)\left[N_Y^0 + \int_0^t {\rm d}\tau \frac{\Gamma_Y(\tau) N_Y^{\rm eq}(\tau)}{S_{\rm QGP}(\tau)}\right], \quad (5)$$

where

$$S_{\rm QGP}(t) = \exp\left[-\int_0^t {\rm d}\tau \Gamma_Y(\tau)\right] \quad (6)$$

is the QGP suppression factor representing the probability that an Y, present at $t = 0$, has survived at time t, and N_Y^0 is the number of primordially produced Y's after pre-equilibrium (nuclear) absorption.

The solution to the rate Eq. (3) requires the time dependence of the temperature, $T(t)$. To this end, we describe the space-time evolution of the system with a simple thermal fireball expansion [38]. It is constructed to reproduce the main features (timescales and transverse flow velocities) of hydrodynamical simulations of A-A collisions [39], and has been applied before to thermal dilepton [40] and charm(onium) [18, 31] production at SPS and RHIC energies, cf. App. B for more details. The resulting temperature profiles are summarized in Fig. 6: the pure QGP phase lasts for about 3 fm/c at RHIC with initial temperatures, T_0, close to 400 MeV, while its duration is $\sim$8 fm/c at LHC with $T_0 = T(\tau_0) \simeq 1$ GeV.

The final ingredient needed for the solution of the rate Eq. (3) is the equilibrium number, $N_Y^{\rm eq}$, of Y states, governing their regeneration contribution throughout the evolution. As elaborated in App. C, for a fixed number of $b\bar{b}$ pairs in the system, $N_Y^{\rm eq}$ depends on the spectrum of open-bottom states in the QGP. We consider the following possibilities:
(i) b quarks with $m_b = 5.280$ GeV,
(ii) b quarks with in-medium mass $m_b(T)$ following from the relation

$$2m_b(T) = m_Y + \varepsilon_B^Y(T) \quad (7)$$

with constant (free) Y masses and binding energies according to Fig. 3,
(iii) B hadrons as listed by the particle data group [26], and
(iv) open-bottom hadrons as extrapolated from known charmed hadrons.
The general trend is that a higher degeneracy and a smaller mass of available open-bottom states favors b and $\bar{b}$ quarks to reside in the former and thus entails a smaller equilibrium abundance of bottomonia, as reflected in Fig. 7 (cf. also App. C 1).

So far our discussion has been residing on the assumption that open-bottom states have momentum distributions in thermal equilibrium with the bulk matter. However, due to the rather short duration of a few fm/c of the QGP phase in URHIC's, and a b-quark mass that exceeds expected early temperatures by a large factor, this is presumably not a realistic assertion [17, 18]. Following a suggestion made in Ref. [31], all our results displayed in the main text below therefore contain a schematic correction to account for incomplete b-quark equilibration, see App. C 2, with the pertinent thermal relaxation times taken from Refs. [17, 18] which in turn provide a reasonable description of recent RHIC data for single-electron spectra (attributed to D and B meson decays) [41, 42]. The associated numerical uncertainty is illustrated by considering the thermal-equilibrium limit in App. E.

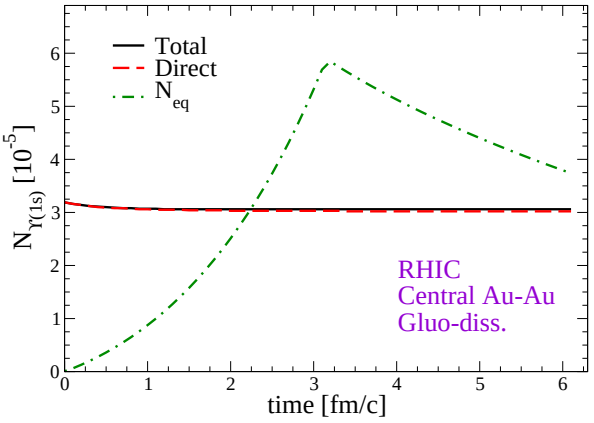

FIG. 8: (Color online) Υ(1s) abundance as a function of time for central (b = 1 fm) Au-Au collisions at RHIC using the gluo-dissociation process (without feeddown from excited states). The solid line includes Υ suppression and regeneration and is almost indistinguishable from the dashed line corresponding to Υ suppression only. The dash-dotted line represents the Υ-equilibrium number which governs the regeneration term in Eq. (4).

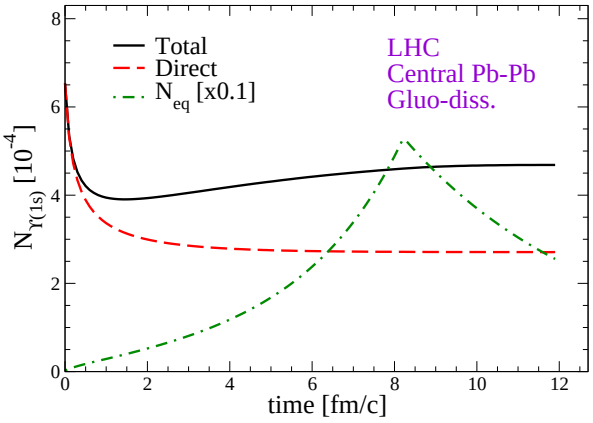

FIG. 9: (Color online) Υ(1s) abundance as a function of time for central (b = 1 fm) Pb-Pb collisions at LHC using the gluo-dissociation suppression mechanism (without feeddown from higher bottomonium states). The solid line, including both suppression and regeneration, indicates substantial secondary Υ production when compared to the dashed line (no gain term), facilitated by rather large Υ-equilibrium numbers (dash-dotted line) and reaction rates.

B. Time Evolution of Υ in Central A-A

With all ingredients in place we proceed to evaluate the time evolution of the number of Υ states in central Au-Au (Pb-Pb) collisions by convoluting the rate equation (3) over the thermal fireball expansion. As a reference scenario commonly used in the literature, we first consider Υ interactions using the gluo-dissociation process with vacuum-binding energies. We then turn to our default scenario corresponding to the quasifree mechanism with in-medium binding energies.

1. *Gluo-Dissociation*

As elaborated in Sec. III B, in the gluo-dissociation scenario we are limited to using vacuum-binding energies which we define relative to the hadronic open-bottom threshold. This amounts to equating the bottom-quark mass, m_b, to the mass of the lightest bottom hadron, *i.e.*, $m_b = m_B = 5.280$ GeV. This rather large mass entails comparatively large Υ-equilibrium numbers (cf. dash-dotted lines in Fig. 8 (RHIC) and 9 (LHC)), which for both RHIC and LHC significantly exceed primordial production in the later stages of the evolution.

Nevertheless, at RHIC the effect of regeneration is essentially irrelevant (full vs. dashed line in Fig. 8) due to small reaction rates at the relevant temperatures of $T < 400$ MeV, cf. Fig. 2.

The situation is different at LHC (Fig. 9) where secondary production is found to be at the 40% level (dashed vs. full line Fig. 9), due to a combination of a longer plasma lifetime (facilitating the build-up of a larger "equilibrium" limit due to thermal relaxation of b quarks) as well as the higher initial temperatures where the inelastic reaction rates are much increased (cf. Fig. 2). However, within the gluo-dissociation framework the importance of regeneration at LHC crucially hinges on the large Υ-equilibrium abundance induced by the large mass of the bottom quark, $m_b = 5.280$ GeV, which in turn was used to consistently implement the vacuum binding energy of the Υ. This behavior will be modified if in-medium binding energies are employed, as we will see in the following subsection.

2. *Quasifree Dissociation*

As discussed above, we use the quasifree approach to inelastic reaction rates to implement in-medium reduced Υ binding energies following the estimates within a screened heavy-quark (Cornell) potential of Ref. [33]. Imposing Eq. (7) further entails appreciably reduced bottom-quark masses with correspondingly smaller Υ-equilibrium numbers (see full line in Fig. 7). This, in turn, leads to $N_\Upsilon^{\rm eq}$ being well below the initial hard production at both RHIC and LHC. At the same time, the reaction rates are much increased over the free gluo-dissociation scenario of the previous section.

At RHIC, the Υ-equilibrium number is so small that secondary production is virtually absent, cf. dashed vs. solid line in Fig. 10. However, the increased inelastic reaction rates lead to an appreciable suppression of nearly 50% of the initial number (after nuclear absorption). This rather dramatic effect is almost entirely due to the reduced Υ binding energy induced by a screening of the b-$\bar{b}$ potential in the QGP (the binding energy is already reduced to $\sim$550 MeV at T_c, rapidly dropping

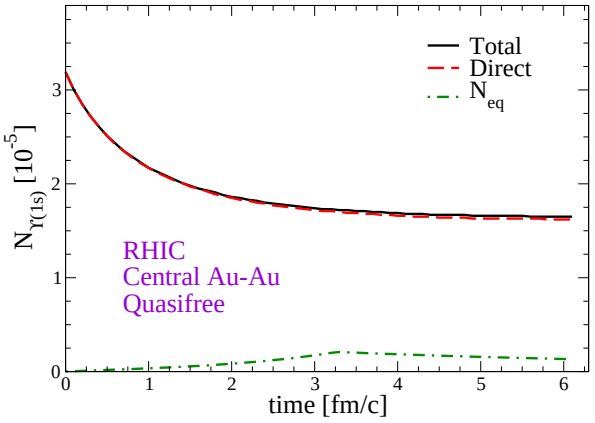

FIG. 10: (Color online) Υ(1s) abundances as a function of time for central (b = 1 fm) Au-Au collisions at RHIC using the quasifree suppression mechanism with in-medium reduced binding energies (no feeddown from higher bottomonia included). The solid line (Υ suppression and regeneration) is similar to the dashed line (Υ suppression only). This is a consequence of the small Υ-equilibrium abundances (dash-dotted line).

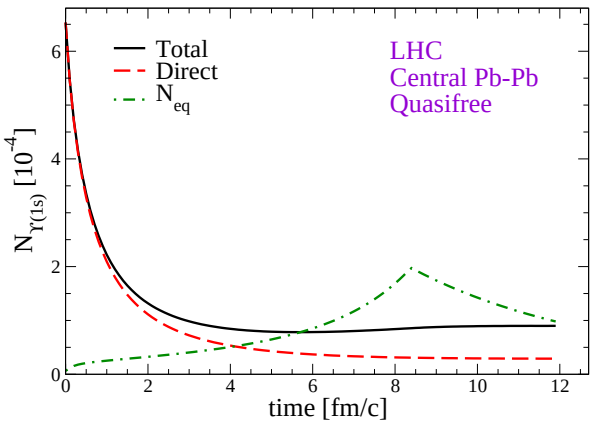

FIG. 11: (Color online) The same as Fig. 10 but for central (b = 1 fm) Pb-Pb collisions at LHC. While the total yield (solid line) builds up a large fraction of regenerated Υ's (due to noticeable equilibrium abundances (dash-dotted line)), the prevalent feature is a net suppression by about a factor of 7.

further before reaching zero at approximately 4.3 T_c). Thus, the magnitude of Υ suppression at RHIC appears to be a rather sensitive measure for Debye screening of the in-medium heavy-quark potential. The effects become stronger at LHC, cf. Fig. 11. Despite a significant increase of the final Υ number due to regeneration in central collisions (solid vs. dashed line), the overall effect is an almost sevenfold suppression of the primordial yield (after nuclear absorption), which again is mostly facilitated by an increased reaction rate originating from a reduced binding energy, especially in the early phases.

We furthermore check the sensitivity of our LHC calculation to the input of the charged-particle multiplicity which is controlled by the total entropy in the fireball,

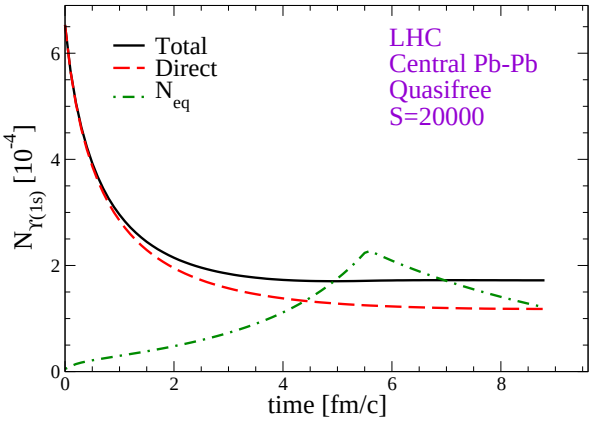

FIG. 12: (Color online) Same as Fig. 11 but with a total entropy of the fireball reduced to half (S=20000), corresponding to a charged-particle multiplicity per unit rapidity of about ∼1600.

cf. App. B. Reducing S (and therefore $\mathrm{d}N_{\mathrm{ch}}/\mathrm{d}y$) by a factor of 2 and keeping everything else the same amounts to smaller initial temperatures (by a factor $\sim 2^{1/3}$), shorter lifetimes of QGP (5.5 fm/c vs. 8.5 fm/c; the duration of the mixed phase is changed very little) and smaller volumes. The latter imply larger open-bottom densities at given T and thus an increase (by a factor of 2) of the open-bottom fugacity, γ_b, which in turn increases the equilibrium limit of the bottomonium number by that same factor. On the other hand, the smaller temperatures and lifetimes of the evolution also inhibit the thermal relaxation of bottom quarks, which reduces the correction factor $\mathcal{R}$ of Eq. (C7). The combination of these two effects leads to an equilibrium number which both in magnitude and time-dependence is quite similar to the evolution scenario with the larger $\mathrm{d}N_{\mathrm{ch}}/\mathrm{d}y \simeq 3200$ (S=40500). The main net effect is thus the less efficient dissociation due to the smaller temperatures in the evolution leading to a final suppression factor (relative to the initial yield after nuclear absorption) of ∼1/4 for $\mathrm{d}N_{\mathrm{ch}}/\mathrm{d}y \simeq 1600$ as compared to ∼1/7 for $\mathrm{d}N_{\mathrm{ch}}/\mathrm{d}y \simeq 3200$. Furthermore, the final yield is now dominated by the suppressed direct contribution.

We also note that at both RHIC and LHC most of the suppression occurs in the first 2-3 fm/c, underlining that Υ production is an observable which is sensitive to early (QGP) phases of central heavy-ion reactions.

3. *Comparison to Charmonium*

It is worthwhile to confront the bottomonium results with the ones for charmonium of our previous analysis along similar lines [7, 10]: when going from SPS to RHIC energies, we have predicted a transition from a charmonium suppression-dominated regime at SPS to mostly regeneration at RHIC, with an approximately constant net suppression relative to initial production. The situation

for bottomonium found here is quite different: in scenarios with color screening we expect the dominant mechanism to be Υ suppression both at RHIC and LHC, which increases with collision energy. This suggests the interesting possibility of observing an absence of suppression (or even enhancement over initial production [11]) for charmonium at LHC [11] together with substantial suppression of bottomonium which would provide a rather unambiguous signature of charmonium regeneration in particular, and QGP formation (including screening) in general. A similar feature (albeit less pronounced) might also be present at RHIC if color-screening and associated reduction in Υ binding energies become operative below temperatures of $\sim 2T_c$: in central Au-Au a 50% suppression of (the much more tightly bound) Υ (after nuclear absorption) should be compared to a 30% net suppression of J/ψ's after inclusion of the (prevalent) regeneration.

We emphasize again that the magnitude of the net Υ suppression is quite sensitive to the strength of color screening (affecting the bottomonium binding energies, and, in turn, the b-quark mass according to $m_b = (m_Y + \varepsilon_B)/2$): at both RHIC and LHC the scenario without screening (Figs. 8 and 9) leads to little net suppression (contrary to Figs. 10 and 11 where screening is included). At RHIC, this is due to the larger binding energies leading to a factor of $\sim$10 decrease in the reaction rates around $T = 300$ MeV, while at LHC it is due to larger b-quark masses implying larger Y equilibrium abundances which facilitate the regeneration in the early phases. On the other hand, uncertainties in the implementation of the screening mass (*e.g.*, using $\mu_D = \sqrt{1+N_f/6}\,gT$ with N_f=3 rather than the default $\mu_D = gT$) are small (less than 15% for the final abundances). We recall that all considerations so far concern the exclusive Υ yields in central A-A collisions.

C. Excited Bottomonia and Feeddown

A complete description of inclusive Υ production requires to account for feeddown contributions from (late) decays of higher bottomonium states. Thus, one also needs to determine the (in-medium) production systematics of these states. In addition, it is expected that some excited bottomonia may be measured directly, providing further model tests. According to Ref. [24] and previous experimental studies of bottomonium systems at Fermilab [43], the final Υ yield observed in $p\bar{p}$ collisions at $\sqrt{s_{NN}} = 39$ GeV is composed of up to 50% from feeddown, see Tab. I. For simplicity, we will in the following neglect Υ(3s) states and will not distinguish between χ_b states. We will also assume that the composition of the primordial Υ yield is energy- and system-size independent.

The dissociation rates for Υ' and χ_b are evaluated within the quasifree formalism including in-medium binding energies following the screening estimates of Ref. [33] (amounting to $\varepsilon_B \simeq$150-200 MeV at T_c, reaching zero at about 1.8 T_c), cf. Figs. 3 and 5 (recall from Sec. III B that the gluo-dissociation approach cannot be applied to the small binding energies at hand and therefore does not allow for a consistent treatment of feeddown effects). For illustration purposes, we display in Fig. 13 the pertinent suppression factors, Eq. (6), for central Pb-Pb collisions at LHC (neglecting the gain term in the rate equation (3)). The Υ' and the χ_b exhibit similar suppression (dashed and dash-dotted (χ_b) line, respectively), almost a factor of 10 stronger than for Υ mesons (solid line), which is, of course, due to their smaller binding energies.

prompt $\Upsilon(1s)$	$\sim 51\%$,
$\Upsilon(1s)$ from $\chi_b(1P)$ decays	$\sim 27\%$,
$\Upsilon(1s)$ from $\chi_b(2P)$ decays	$\sim 10\%$,
$\Upsilon(1s)$ from $\Upsilon(2s)$ decays	$\sim 11\%$,
$\Upsilon(1s)$ from $\Upsilon(3s)$ decays	$\sim 1\%$.

TABLE I: Decomposition of the inclusive Υ yield into prompt and feeddown contributions from excited bottomonia in $p\bar{p}$ collisions at $\sqrt{s_{NN}} = 39$ GeV [43].

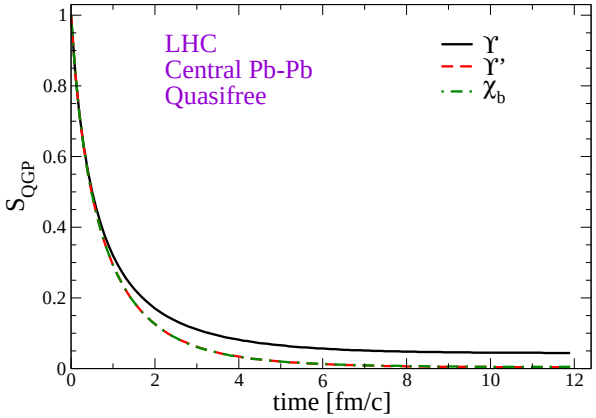

FIG. 13: (Color online) QGP suppression of bottomonia in central (b = 1 fm) Pb-Pb collisions at LHC, using the quasifree destruction process. Solid line: Υ, dashed line: Υ', dash-dotted line: χ_b.

The much stronger suppression of excited bottomonia (as well as their smaller equilibrium limits) compared to direct Υ's has important consequences for the inclusive Υ yields at both RHIC and LHC which will be shown in the following section. For central A-A collisions, the suppression in inclusive Υ production is about 30-40% more pronounced than for exclusive yields as displayed in Sec. IV.

V. CENTRALITY DEPENDENCE

The results presented in the previous sections were calculated for central collisions (b = 1 fm). In this section, we extend our results to different centrality classes by

solving the rate Eq. (3) for Au-Au (Pb-Pb) collisions for various impact parameters, b, (as was done before for charmonia in Ref. [7]), and then plotting the yields at the end of each time evolution as a function of the number of nucleon participants, $N_{\rm part}(b)$.

To solve the rate equations, we focus on the inelastic reaction rates obtained from the quasifree suppression mechanism for b quarks in the QGP with in-medium mass $m_b(T)$ (corresponding to the lower set of curves in Fig. 5) and include thermal off-equilibrium corrections for $N_\Upsilon^{\rm eq}(t)$ [according to eq. (C7)]. The inclusive Υ yields account for the feeddown from Υ' and χ_b for which we solve the same rate Eq. (3) with pertinent reaction rates. The primordial numbers of $b\bar{b}$ pairs and bottomonia (the latter subjected to an identical but centrality-dependent nuclear absorption) are obtained by scaling our input numbers of Sec. II according to the number of binary collisions, $N_{\rm coll}(b)$ (characteristic for hard processes).

The centrality dependence of the fireball evolution (App. B) is constructed assuming the total entropy at given impact parameter to be proportional to $N_{\rm part}(b)$, $S_{\rm tot}(b) \propto N_{\rm part}(b)$ (characteristic for soft processes, which for RHIC data is approximately satisfied within 20% or so; for LHC the uncertainty is larger due to competing effects anticipated from gluon saturation and an increasing importance of an $N_{\rm coll}$-component [44]). The initial transverse radius (r_0) is estimated in cylindrical symmetry from the nuclear overlap function with constant formation time, tranverse acceleration and longitudinal velocity, cf. Eq. (B1) (for the purpose of extracting the temperature and volume evolution, effects of finite ellipticities in noncentral collisions are not significant).

In the following, we first study the centrality dependence of the Υ yield at RHIC, then at LHC, and finally the Υ'/Υ ratio.

A. RHIC

Fig. 14 shows our results for Υ production in $\sqrt{s_{NN}} =$ 200 GeV Au-Au as a function of participant number, normalized to the number of binary collisions. As expected from the dependencies in Fig. 10, the Υ yield (solid line) exhibits a substantial increase in suppression going from peripheral to central collisions, with negligible regeneration (dash-dotted line), *i.e.*, the final Υ yield is exclusively due to primordial production subject to suppression in the QGP (dashed line). This is primarily a consequence of the small number of $b\bar{b}$ pairs created in hard nucleon-nucleon scatterings, implying an Υ equilibrium number which is well below the actual number at any time (more so toward peripheral collisions). The prevalent effect is thus a significant suppression of the inclusive Υ yield with centrality, originating from (i) suppression of direct Υ's due to (substantial) color screening, and (ii) suppression of (less bound) excited bottomonia with subsequent feeddown. We recall that, due to the irrelevance of regeneration effects, uncertainties in the nuclear absorption-cross section directly reflect itself in the total yield (*e.g.*, if the absorption-cross section is reduced by a factor of 2 (*i.e.*, from 3.1 mb to 1.55 mb), the nuclear absorption factor is reduced to its square root (*i.e.*, from 0.68 to 0.82 for central Au-Au), and the corresponding percentage change (+20%) carries over to the total yield).

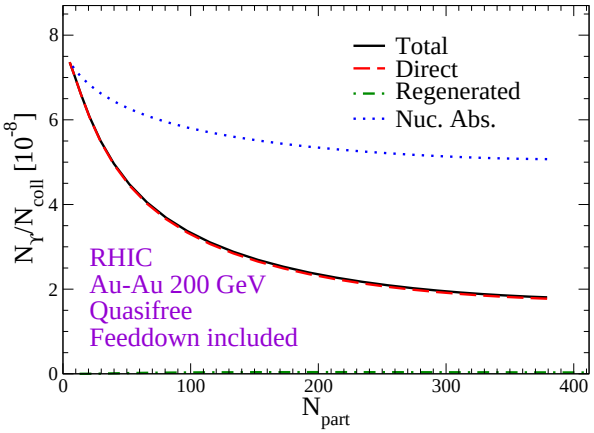

FIG. 14: (Color online) Centrality dependence of $N_\Upsilon/N_{\rm coll}$ at RHIC (Au-Au collisions at $\sqrt{s_{NN}} = 200$ GeV) using the quasifree suppression mechanism including color screening. Dotted line: Υ after nuclear absorption; dashed line: suppressed primordial Υ; dash-dotted line: regenerated Υ; solid line: total Υ.

Overall, our findings for Υ production at RHIC are rather reminiscent of the J/Ψ suppression pattern at SPS as calculated in a similar approach [7] (in line with NA50 data [45]).

B. LHC

In Fig. 15 we present our predictions for the centrality dependence of the Υ yield at LHC within the same approach as for RHIC. The longer lifetime of the QGP phase and, in particular, the higher temperatures reached at LHC render the suppression of primordial Υ (dashed line) even more pronounced. Regeneration (dash-dotted line), however, is no longer negligible, accounting for up to 2/3 of the final yield in central collisions (implying that there is very little uncertainty related to the nuclear absorption cross section). This should leave further traces in p_t-dependencies, such as a softening of the spectra and a sizable v_2. Nevertheless, the situation at LHC is qualitatively similar to the one at RHIC as far as the centrality dependence is concerned, *i.e.*, the prevailing manifestation of QGP formation is Υ suppression at *both* RHIC and LHC.

We also illustrate again the impact of a smaller charged-particle multiplicity in Pb-Pb at LHC, leaving all other quantities unchanged, see Fig. 16. As found for the time dependence in central collisions (Sec. IV B 2), the smaller initial temperatures and QGP lifetimes lead to a factor of ∼2 less suppression. Also note that the

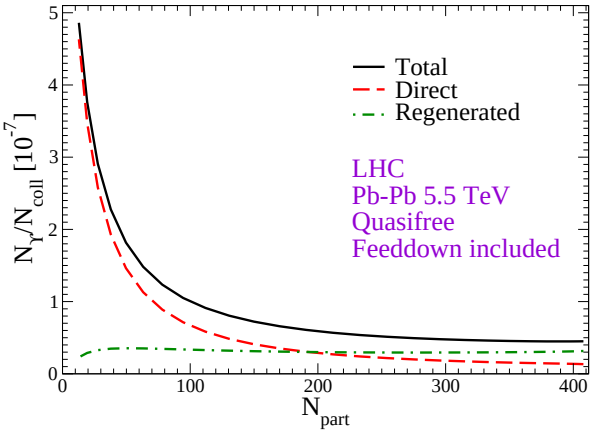

FIG. 15: (Color online) Same as Fig. 14, but for Pb-Pb collisions at LHC ($\sqrt{s_{NN}} = 5.5$ TeV) with $\mathrm{d}N_{\mathrm{ch}}/\mathrm{d}y|_{\mathrm{central}} \simeq 3200$.

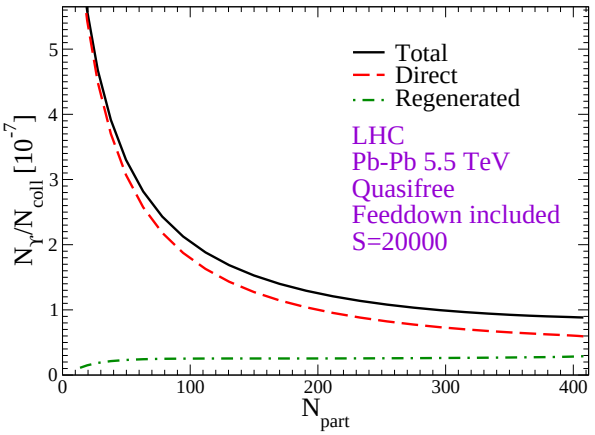

FIG. 16: (Color online) Same as Fig. 15, but with half the total entropy in the fireball at each impact parameter, corresponding to $\mathrm{d}N_{\mathrm{ch}}/\mathrm{d}y \simeq 1600$ in central collisions.

absolute number of regenerated Υ's hardly changes, implying that the final yield is now dominated by the primordial component.

C. Υ'/Υ ratio

We finally extract the Υ'/Υ ratio at LHC which was already implicit in the centrality dependence of the inclusive Υ yield shown in the previous section. The smaller Υ' binding energy obviously facilitates its suppression, and its larger mass additionally inhibits regeneration (due to smaller equilibrium abundances). Consequently, we find a decreasing Υ'/Υ ratio, by about a factor of 2 (3) when going from peripheral (p-p) to central collisions, cf. Fig. 17 (feeddown to the Υ' has been neglected; note that the limit for p-p amounts to 33%, or 17% upon inclusion of the dilepton decay branching ratios). We note that even for central collisions, our calculations amount to a ratio of Υ'/Υ ~9% which lies well above its thermal-

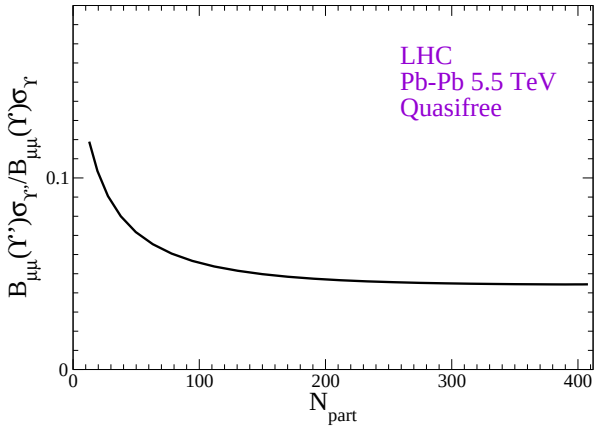

FIG. 17: (Color online) Centrality dependence of $N_{\Upsilon'}/N_\Upsilon$ (supplemented by the dilepton-branching ratios of $B_{\mu\mu}(\Upsilon')$~1.3% and $B_{\mu\mu}(\Upsilon)$~2.5%, respectively; feeddown on Υ' states is not included) at LHC for Pb-Pb collisions at $\sqrt{s_{NN}} = 5.5$ TeV.

equilibrium value of ~5% (at $T = 180$ MeV) that one would expect if bottomonium states were entirely created via statistical hadronization [46]. The reason is that the number of Υ' reaches its terminal value at the beginning of the mixed phase where the pertinent reaction rate, $\Gamma_{\Upsilon'}$, becomes small, while the equilibrium limit drops by a factor of two toward the end of the mixed phase (as for the Υ in Fig. 11). On the other hand (see also Fig. 11), the terminal number of Υ essentially happens to coincide with the equilibrium value at the end of the mixed phase (even though it is frozen much earlier). Therefore the final Υ'/Υ ratio is roughly a factor two larger than the equilibrium value at the end of the mixed phase, which is the result displayed in Fig. 17 for central collisions.

VI. CONCLUSIONS

At heavy-ion colliders (RHIC and LHC) hadrons containing bottom quarks are expected to become an important new probe of the produced (novel) forms of strongly interacting matter. In this article we have presented a kinetic theory framework to assess the evolution of bottomonia in the QGP phases of high-energy heavy-ion reactions, neglecting any reinteractions in hadronic matter (which is presumably a fair approximation for Υ, χ_b and Υ' states). The underlying rate equation requires several inputs: (1) initial bottomonium abundances (which we estimated from collision-scaled p-p data), (2) space-time evolution of temperature (for which we employed an expanding fireball model), (3) inelastic reaction rates of bottomonia, and (4) bottomonium equilibrium abundances.

For the inelastic reaction rates we have evaluated two mechanisms for dissociation due to thermal light quarks and gluons in the QGP: (i) gluo-absorption (the analogue of photo-dissociation) and (ii) "quasifree" scattering of

both quarks and gluons off individual b and $\bar{b}$ quarks in the bound state. Whereas processes of type (i) are appropriate (and expected to be dominant) for deeply bound quarkonia, processes (ii) allow to treat the case of small binding energies (where gluo-dissociation leads to anomalously small reaction rates). Consequently, when introducing effects of color screening, the associated (temperature-dependent) reduced binding energies mandate the use of the quasifree processes, while for vacuum binding energies gluo-dissociation is employed.

The equilibrium limits of bottomonia, which govern the gain term (regeneration) in the rate equation, follow the trends previously established for charmonia: for a fixed number of $b\bar{b}$ pairs in the system (at given centrality), larger masses (and smaller degeneracies) of open-bottom states imply larger Y-equilibrium limits (rendering bottomonium formation more favorable). However, in most cases considered (in particular when implementing medium effects with relatively small b-quark masses) the equilibrium limit was significantly below the initial value from hard production (after nuclear absorption), especially after applying a schematic correction for incomplete b-quark thermalization.

Our main results may therefore be summarized as follows: (I) color screening (*i.e.*, in-medium reduced binding energies) leads to a substantial increase of the inelastic bottomonium reaction rates; (II) at RHIC, this manifests itself as a 50% suppression effect (factor $\sim$2) in the QGP phase (with virtually no regeneration), whereas for vacuum-Υ states almost no (thermal) suppression occurs (in which case suppression in inclusive yields is due to feeddown from excited states); (III) at LHC, assuming $\mathrm{d}N_{\mathrm{ch}}/\mathrm{d}y \simeq 3200$ in central Pb-Pb, the net QGP suppression becomes substantially stronger (factor $\sim$7 (1.4) for in-medium (vacuum) binding energies), with the final yield containing a 75% (30%) component of regenerated Υ's. If the charged-particle multiplicity turns out to be smaller (*e.g.*, $\mathrm{d}N_{\mathrm{ch}}/\mathrm{d}y \simeq 1600$), the reduced QGP initial temperature and lifetime will lead to weaker net suppression (*e.g.*, factor $\sim$2 less).

Our general finding is thus that in heavy-ion reactions at *both* RHIC and LHC, Υ suppression is the prevalent effect as a function of collision centrality, and there is large sensitivity to color screening in the QGP. This is quite different from our previous studies of charmonia where J/Ψ regeneration is expected to be the dominant mechanism for RHIC energies and above.

Concerning future improvements, it is desirable to provide a more accurate treatment of in-medium bottomonium properties, implementing both screening and dissociation processes, as well as non-thermal b-quark distributions, simultaneously in a more microscopic approach.

Acknowledgments

This work was supported in part by the U.S. National Science Foundation through a CAREER award (RR and HvH) under Grant No. PHY-0449489 and through a REU program (SL) under Grant No. PHY-0354098. One of us (HvH) thanks the Alexander von Humboldt foundation (Feodor-Lynen program) for partial support. One of us (LG) was supported by the Director, Office of Energy Research, Office of High Energy and Nuclear Physics, Divisions of Nuclear Physics, of the U.S. Department of Energy under Contract No. DE-AC02-05CH11231.

APPENDIX A: BRIEF REVIEW OF LATTICE QCD RESULTS

Finite-temperature lQCD calculations exhibit a substantial reduction of the heavy-quark free energy [47, 48],

$$F_{Q\bar{Q}}(r,T) = U_{Q\bar{Q}}(r,T) - T\,S_{Q\bar{Q}}(r,T)\ , \qquad \text{(A1)}$$

with increasing temperature. When implementing the free energy into a Schrödinger equation, J/ψ (ψ') mesons have been found to dissolve slightly above (below) T_c [49]. More recently, it has been argued that the internal energy, $U_{Q\bar{Q}}$, is the more appropriate quantity to be identified with a potential. Corresponding solutions to the Schrödinger equation entail significantly larger dissociation temperatures of the J/ψ of around $T_{\mathrm{diss}}\simeq 2T_c$ [34, 50, 51, 52]. This led, in fact, to better consistency with (quenched) lQCD results for charmonium spectral functions, in which the peak structures associated with the lowest-lying resonances (J/ψ and η_c) disappear slightly below $2T_c$ [2, 3, 4]. With the mass (peak position) of the spectral functions approximately staying constant [53], the key property of the charmonium spectral functions is thus a change in their widths, *i.e.*, inelastic reaction rates. This is further corroborated by lQCD studies which find the J/ψ width to increase across the phase transition, from very small below to about 200 MeV just above T_c [53]. Such a behavior is quite consistent [37] with both hadronic-model calculations below T_c, which typically result in small inelastic reaction rates of $\lesssim$0.1 fm^{-1} (mostly due to $\pi, \rho + J/\psi$ breakup) [54], and parton-induced destruction above T_c, typically of the order of 1 fm^{-1}. Also note that in the presence of color screening, which induces a reduction in the c-$\bar{c}$ binding energy ($\epsilon_B > 0$), a constant charmonium mass implies a decrease in the open-charm threshold, according to the relation

$$m_\Psi = 2m_c - \varepsilon_B\ . \qquad \text{(A2)}$$

A decrease in the open-charm threshold with T has indeed been found in the lQCD free energies (or potentials), at least above T_c [55], and complies naturally with an increase in the bound-state width, due to larger phase space in the break-up reactions, *e.g.*, $g + J/\psi \to c + \bar{c}$.

Effects of the hadronic phase are neglected in this article; first lQCD results [56] (as well as potential models based on lQCD [50]) indeed indicate much higher dissociation temperatures of the Υ than for J/ψ, around $T_{\rm diss}^{\Upsilon} \simeq 4T_c$.

APPENDIX B: THERMAL FIREBALL PARAMETERIZATION

The starting point for the thermal fireball model is a cylindrical ansatz for the (proper) time dependence of the (isotropic) three-volume according to

$$V_{\rm FB}(t) = (z_0 + v_z t)\,\pi \left(r_0 + \frac{a_\perp}{2} t^2\right)^2 \ . \qquad \text{(B1)}$$

The longitudinal expansion is characterized by (i) an expansion velocity of $v_z = 1.4c$ representing a rapidity range of $\Delta y \simeq 1.8$ typical for a thermal fireball width, and (ii) an initial length $z_0 = 0.6$ (0.125) fm for RHIC (LHC) which carries the meaning of a formation (thermalization) time, $\tau_0 = z_0/\Delta y$ =0.33 (0.07) fm/c at RHIC (LHC). The initial transverse size is determined by the centrality of the collision, *e.g.*, $r_0 = 6.4$ (6.6) fm for $b = 1$ fm Au-Au (Pb-Pb) collisions at RHIC (LHC).

If one further assumes the total entropy, S, of the system to be conserved (*i.e.*, isentropic expansion), the temperature evolution of the fireball matter can be inferred by equating the entropy density to the one of a thermal medium. For a non-interacting QGP one has

$$\begin{aligned} s(t) &= \frac{S}{V_{\rm FB}(t)} \\ &\equiv \mp \sum_i d_i \int \frac{{\rm d}^3k}{(2\pi)^3} \big\{ \pm f_i(\omega_i) \ln[f_i(\omega_i)] \\ &\quad + [1 \mp f_i(\omega_i)] \ln[1 \mp f_i(\omega_i)] \big\} \ , \end{aligned} \qquad \text{(B2)}$$

where f_i denote the Fermi-Dirac (i=q, $\bar{q}$, upper signs) or Bose-Einstein (i=g, lower signs) distribution functions of (massive) quarks or gluons with on-shell energies $\omega_i = \sqrt{k^2 + m_i^2}$ (m_i: thermal mass), and d_i stand for the pertinent spin-color-flavor degeneracies. We will consider two scenarios for the QGP equation of state: (i) massless partons with an effective number of quark flavors $N_f = 2.5$; in this case, $s = (d_g + 10.5 N_f) 4\pi^2 T^3/90$, and the temperature can be obtained explicitly as $T(t) = {\rm const} \times (S/V_{FB}(t))^{1/3}$; (ii) a three-flavor QGP with thermal parton masses,

$$m_{u,d}^2 = \frac{g^2T^2}{6}, \quad m_s^2 = m_0^2 + \frac{g^2T^2}{6}, \quad m_g^2 = \frac{3}{4} g^2 T^2, \qquad \text{(B3)}$$

where m_0=150 MeV is taken as a bare strange-quark mass; in this scenario, Eq. (B2) provides an implicit relation for $T(t)$ which is solved numerically. However, we observe no significant differences for the temperature profiles when calculating the entropy density for a QGP with massless degrees of freedom (and $N_f = 2.5$) or massive partons according to Eq. (B3).

If the entropy density, $s(t)$, drops below the critical value of the QGP phase, $s_c^{\rm QGP} \equiv s^{\rm QGP}(T_c = 180$ MeV), we perform the standard mixed-phase construction,

$$\frac{S}{V_{\rm FB}(t)} = f s_c^{\rm HG} + (1-f) s_c^{\rm QGP} \qquad \text{(B4)}$$

with volume fractions f and $1-f$ of matter in the hadron gas (HG) and QGP, respectively. The entropy density of the HG at T_c, $s^{\rm HG}(T_c) \simeq 6.1$ fm^{-3}, is computed from a HG including all resonances up to masses of about 2 GeV, with a baryonic chemical potential $\mu_B \simeq 30$ (2) MeV corresponding to (expected) chemical freezeout at RHIC (LHC). The charged-particle multiplicity is then determined by fixing the total entropy of the system [38], *e.g.*, S=10000 (40500) for central collisions at RHIC (LHC) translating into ${\rm d}N_{\rm ch}/{\rm d}y \simeq 800$ (3200; we have evaluated an LHC scenario with S=20000, *i.e.*, ${\rm d}N_{\rm ch}/{\rm d}y \simeq 1600$, which is closer to extrapolations based on present RHIC data [11, 57]). As mentioned above, we neglect the hadronic evolution of the system.

APPENDIX C: EQUILIBRIUM ABUNDANCES

Following our assumption of a fixed number of b-$\bar{b}$ pairs (at given centrality) in the fireball, the Y-equilibrium number not only depends on temperature and volume, but also on a bottom-quark fugacity $\gamma_b \equiv \gamma_{\bar{b}}$ via

$$N_Y^{\rm eq}(T) = d_Y\, \gamma_b(T)^2\, V_{\rm FB}(t) \int \frac{{\rm d}^3p}{(2\pi)^3}\, \exp\left(-\frac{E_Y(p)}{T}\right) \qquad \text{(C1)}$$

($E_Y(p) = \sqrt{m_Y^2 + p^2}$, d_Y: spin degeneracy). The temperature dependence of the fugacity is determined by requiring that at each moment the total number of b ($\bar{b}$) quarks in open- and hidden-bottom states matches the primordially produced abundance [9],

$$N_{b\bar{b}} = \frac{1}{2} \gamma_b N_{\rm op} \frac{I_1(\gamma_b N_{\rm op})}{I_0(\gamma_b N_{\rm op})} + \gamma_b^2 N_{\rm hid} \ , \qquad \text{(C2)}$$

where I_j are modified Bessel functions. The numbers of hadronic open and hidden bottom states are given by

$$N_{\rm op}^B \ = \ V_{\rm FB} \sum_X n_X \ , \ X \in \{B, \bar{B}, B^*, \bar{B}^*, \Lambda_b, \ldots\}, \qquad \text{(C3)}$$

$$N_{\rm hid} \ = \ V_{\rm FB} \sum_Y n_Y \ , \ Y \in \{\Upsilon, \chi_{b0}, \chi_{b1}, \ldots\}, \qquad \text{(C4)}$$

respectively, with

$$n_{X,Y} = d_{X,Y} \int \frac{{\rm d}^3p}{(2\pi)^3}\, \exp\left(-\frac{E_{X,Y}(p)}{T}\right) \qquad \text{(C5)}$$

the pertinent densities in Boltzmann approximation ($d_{x,y}$: spin-isospin degeneracy). If the open-bottom

states in the QGP consist of b and $\bar{b}$ quarks, Eq. (C3) is replaced by

$$N_{\rm op}^{b} = V_{\rm FB} \sum_{X} n_X \,, \quad X \in \{b, \bar{b}\} \,. \tag{C6}$$

As emphasized in Ref. [9], for a small number of total $b\bar{b}$ pairs ($N_{b\bar{b}} \lesssim 1$), it is quantitatively important in the determination of γ_b to enforce exact bottom-number conservation (*i.e.*, in each configuration) using the canonical ensemble, which is implemented in Eq. (C2) by the ratio of Bessel functions. For large values of $N_{b\bar{b}}$, the ratio of Bessel functions approaches 1, and one recovers the grand canonical limit. In Eq. (C4), we include all bottomonium states listed in Ref. [26], but due to their relatively large masses compared to B mesons (or bottom quarks), they play no significant role in the determination of γ_b via Eq. (C2). The main uncertainty in this procedure resides in the number, $N_{\rm op}$, of open-bottom states, Eq. (C3) or (C6), which depends on both their masses and degeneracies, as elaborated in the following subsection. Another, more indirect uncertainty in $N_Y^{\rm eq}(T)$ pertains to the assumption of thermal equilibrium of open-bottom states which is underlying Eqs. (C1) through (C6). A pertinent (schematic) correction will be discussed in App. C 2 below.

1. Open-Bottom States in the QGP

To assess the uncertainties associated with the open-bottom spectrum in the QGP we will distinguish two basic scenarios (with one further subdivision each). The first one is that of individual b quarks (with variations in their mass), as to be expected for a weakly interacting QGP. The second one is closer in spirit to a strongly interacting QGP, where (colorless) hadronic correlations persist above T_c. Such a scenario has received renewed attention stimulated by findings of hadronic bound and/or resonance states in lQCD simulations [1, 5] (and effective models [34, 51, 52]) for $T \simeq$ 1-2 T_c. Also, the strong collective phenomena (radial and elliptic flow) found experimentally at RHIC are not easily reconciled within a perturbative framework. On the one hand, we will therefore investigate the survival of hadronic open-bottom states (most importantly B mesons) with a varying degree of level density toward higher masses, *i.e.*, either B meson (and Λ_b baryons) as listed by the particle data group [26] or additional states estimated from analogy to open-charm hadrons (since the expected initial temperatures at LHC are well above $2T_c$, we consider the "hadronic" scenarios only for RHIC). On the other hand, even if no hadronic states are formed in the QGP, at moderate temperatures $T \lesssim 2T_c$, the strong coupling constant α_s may not be small and induce significant temperature-dependences in the in-medium bottom-quark mass due to correlations with surrounding light partons. The main point in the following is that, at fixed $N_{b\bar{b}}$, differences in the open-bottom spectrum affect the b-quark fugacity and thus, in turn, modify the Y-equilibrium abundances. The general mechanism can be summarized as follows [7]: a larger number of available open-bottom states (either due to a large degeneracy or a small mass which facilitates their thermal population) implies a smaller γ_b and thus a smaller equilibrium number of bottomonium states, $N_Y^{\rm eq}$. In other words, heavier (and less) open-bottom states favor b-$\bar{b}$ quarks to reside in bottomonia.

For definiteness, we consider the following four cases for open-bottom states in the QGP, summarized in Fig. 7:

(i) b and $\bar{b}$ quarks with a fixed mass of m_b = 5.280 GeV, corresponding to the mass of the lightest B meson (LHC only, dash-dotted line in Fig. 7);

(ii) b and $\bar{b}$ quarks with in-medium masses $m_b(T)$, where the temperature dependence is inferred in analogy to Eq. (A2) as $2m_b(T) = m_Y + \varepsilon_B^Y(T)$ (Eq. (7)) with the T-dependence of the Υ-binding energy, $\varepsilon_B^\Upsilon(T)$, taken from Ref. [33]. As mentioned above, here and throughout our work we assume all Y masses to be constant. The resulting Υ-equilibrium abundances are indicated by the solid (LHC) and dash-double-dotted line (RHIC) in Fig. 7.

(iii) open-bottom hadrons as listed in the particle data book [26]: Λ_b^0, B, B^*, B_s^0, $B_c^\pm$ (RHIC only, dotted line in Fig. 7).

(iv) open-bottom hadrons including states with estimated masses as extrapolated from systematics of analogous (known) charmed hadrons (RHIC only, dashed line in Fig. 7).

For the two b-quark scenarios (i) and (ii) under LHC conditions (upper two curves in Fig. 7), the main difference amounts to a larger Υ-equilibrium abundance for the larger b-quark mass (case (i)); at high temperatures, where for case (ii) the b-quark mass is essentially half the Υ mass (zero binding energy), the difference is less pronounced due to the flatter thermal distribution functions. Toward smaller temperatures (especially close to T_c), γ_b increases significantly due to a decreasing $N_{\rm op}^b$, and one notices the onset of the effect that, in the canonical ensemble (where b and $\bar{b}$ have to appear together), it becomes increasingly favorable to have a $b\bar{b}$ pair in an Υ state which has a lower mass than separate b and $\bar{b}$ quarks (the vertical decrease of $N_\Upsilon^{\rm eq}$ at T_c is a consequence of the volume expansion during the mixed phase at constant temperature, implying a decrease in γ_b).

At RHIC the b-quark scenarios show a behavior for $N_\Upsilon^{\rm eq}$ analogous to LHC but with reduced magnitude mainly due to the reduction in $N_{b\bar{b}}$. Close to T_c, the scenarios with hadronic open-bottom states, (iii) and (iv), lead to a substantial increase in $N_\Upsilon^{\rm eq}$ over the one with in-medium b-quark mass, since the latter is well below the lowest B meson mass. The sensitivity to higher-mass bottom hadrons becomes more pronounced with

increasing temperature, where they are more easily excited, thus reducing the number of bottomonium states. This, in turn, implies that the b-quark scenario (i), with $m_b = 5.280$ GeV $= m_B$ (not shown in Fig.7), is rather similar to the hadronic scenarios close to T_c.

We finally note that, during the mixed phase (*i.e.*, at T_c), the open-bottom spectrum within each scenario is assumed not to change. With constant temperature and increasing three-volume, $V_{\rm FB}(t)$, this implies that the bottom-quark fugacity, $\gamma_b(T, V_{\rm FB})$, decreases during the mixed phase (since $N_{b\bar{b}}$ is conserved), and with it $N_\Upsilon^{\rm eq}(T, V_{\rm FB})$. The discontinuity in the first derivative of the temperature evolution (cf. Fig. 6) at the beginning of the mixed phase is thus reflected in $\gamma_b(T, V_{\rm FB})$ and $N_\Upsilon^{\rm eq}(T, V_{\rm FB})$.

2. Incomplete b-Quark Thermalization

Due to the rather short duration of a few fm/c of the high-temperature (QGP) phases in URHIC's, and a b-quark mass that exceeds expected early temperatures by a large factor, b-quark thermalization may not be a realistic assertion. Even for charm quarks (an approach to) thermalization appears to be unlikely under RHIC conditions if only perturbative rescattering processes in the QGP are considered [15]. However, recent RHIC data [41] on the elliptic flow of (semileptonic) decay electrons which are attributed to D mesons suggest that charm quarks undergo substantial rescattering [13] in semi-central Au-Au collisions at $\sqrt{s} = 200$ AGeV. A possible microscopic mechanism has been identified in Refs. [17, 18] in terms of resonant c-quark scattering with light antiquarks via D-meson states surviving in the QGP at moderate temperatures, T$\lesssim 2T_c$. It was found that, compared to perturbative calculations, the thermal relaxation times could be reduced by up to a factor of 3-4, thus becoming comparable to the duration of the QGP phase at RHIC. A similar reduction was found for bottom quarks, but with the larger mass implying larger absolute values for the relaxation time scale by a factor of ∼2-3, so that b-quark thermalization remains unlikely at RHIC.

Consequently, the Υ-equilibrium abundances shown in Fig. 7 should be improved by accounting for incomplete thermalization. As in Ref. [31], we here follow a schematic relaxation time approach, by implementing into the thermal equilibrium abundances a reduction factor

$$\mathcal{R} = 1 - \exp\left(-\int \frac{d\tau}{\tau_{\rm eq}}\right), \qquad \text{(C7)}$$

where $\tau_{\rm eq}$ is the bottom-quark equilibration time as obtained within the resonance-scattering model [17]. Typical values of $\tau_{\rm eq}$ range from $\tau_{\rm eq} \simeq 12$ fm/c at $T = 300$ MeV to $\tau_{\rm eq} \simeq 1.1$ fm/c at $T = 1$ GeV, leading to a substantial decrease of the regeneration term in Eq. (3), especially at RHIC. We will illustrate the uncertainties induced by this correction by considering the thermal limit in App. E below.

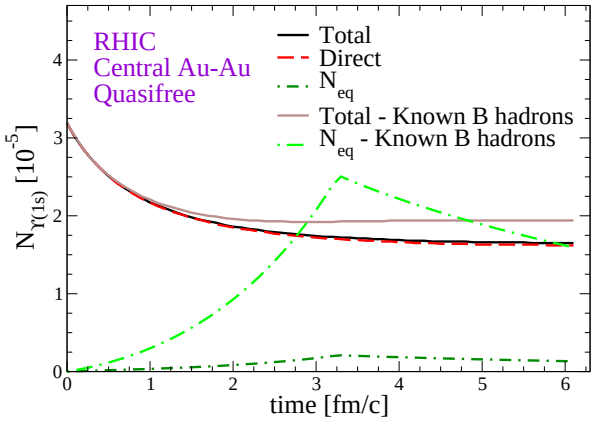

FIG. 18: (Color online) Time evolution of $\Upsilon(1s)$ in central ($b = 1$ fm) Au-Au collisions at RHIC assuming different open-bottom spectra in the QGP. Light curves: open-bottom states constituting known bottom hadrons with the dash-dotted curve showing the Υ-equilibrium abundance and the solid curve indicating the total Υ yield including regeneration. Dark curves: open-bottom states ≡ in-medium b quarks as in Fig. 10.

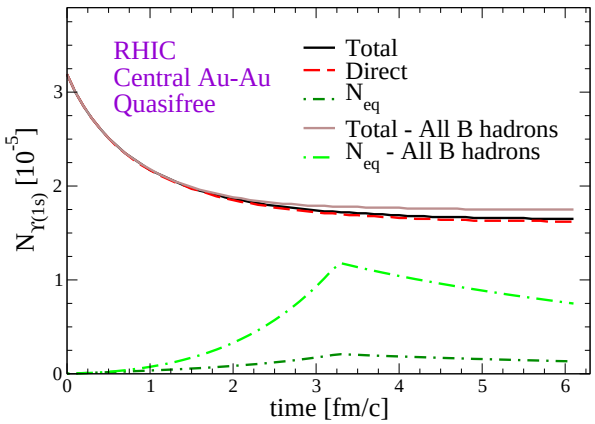

FIG. 19: (Color online) Same as Fig. 18 but assuming a richer (hadronic) open-bottom spectrum in the QGP as estimated from known open-charm hadrons in the vacuum.

APPENDIX D: UNCERTAINTIES DUE TO OPEN-BOTTOM STATES

The dependence of the Υ-equilibrium numbers (without thermal relaxation correction) on different assumptions about the open-bottom spectrum in the QGP was illustrated in Fig. 7 for the following scenarios: (i) b quarks with $m_b = 5.280$ GeV, (ii) b quarks with in-medium mass $m_b(T)$, (iii) B hadrons as listed by the particle data group [26], and (iv) open-bottom hadrons as extrapolated from known charmed hadrons. In this section we study the influence of scenarios (iii) and (iv) on the re-

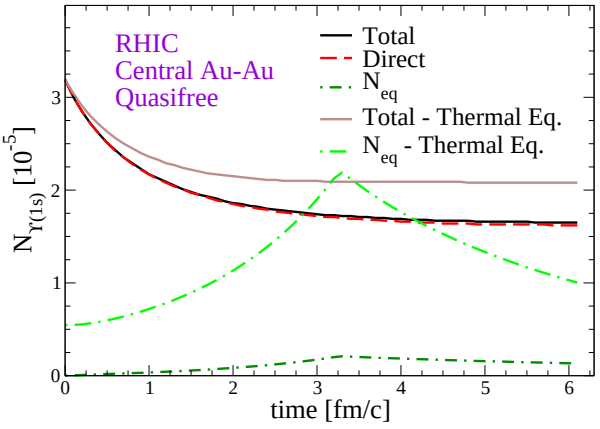

FIG. 20: (Color online) Thermal off-equilibrium effects at RHIC for the suppression of $\Upsilon(1s)$ in central ($b = 1$ fm) Au-Au collisions, using the quasifree process. The light set of curves corresponds to a full thermalization scenario with increased equilibrium abundances (upper dash-dotted line), leading to a 15% component from secondary production (upper solid line). The darker lines correspond to Fig. 10 in the main text.

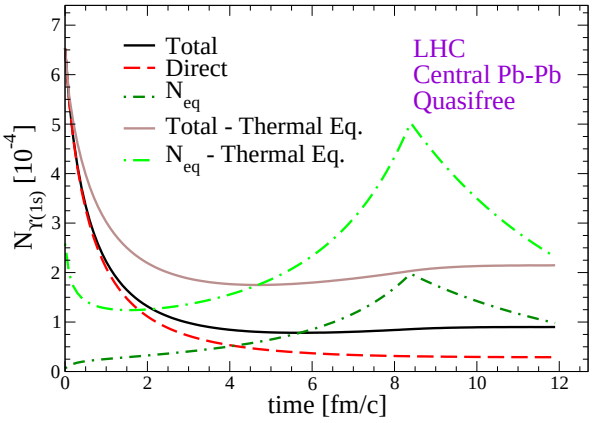

FIG. 21: (Color online) Thermal off-equilibrium effects at LHC for the suppression of $\Upsilon(1s)$ in central ($b = 1$ fm) Pb-Pb collisions, using the quasifree process. The light set of curves indicates our results assuming thermalization of the open-bottom states, showing larger equilibrium abundances (dash-dotted curve) and a larger final Υ yield (solid line) than with thermal off-equilibrium effects (dark set of curves, corresponding to Fig. 11 in the main text).

generation of Υ(1s), restricting ourselves to RHIC energy as it seems unlikely that hadronic correlations would persist at the temperatures anticipated at LHC ($T \lesssim 1$ GeV). We will employ the rates corresponding to quasifree destruction with in-medium binding energies (even though this implies an inconsistency between the rates and the Υ equilibrium number, it will allow us to estimate the maximal possible effect as the quasifree rates are the largest considered in this work). Fig. 18 pertains to the case where the open-bottom states in the QGP are given by the known B-hadron spectrum. Since their mass tends to be larger than the in-medium b quark masses (as used in the main text, cf. Fig. 10), this scenario leads to an increase in the Υ-equilibrium abundances (light vs. dark dash-dotted curves in Fig. 18). However, the overall effect of a slightly enhanced regeneration is small (upper solid line).

If we assume the open-bottom spectrum to follow the same pattern as all known charmed hadrons, the increase in the Υ-equilibrium number over the in-medium b-quark scenario is less pronounced (due to a smaller fugacity, γ_b, relative to using only known B states), and, consequently, also the regeneration, leaving essentially no noticeable effect, cf. Fig. 19.

Thus, overall, the effects of different open-bottom spectra in the QGP on Υ production at RHIC are very small.

APPENDIX E: UNCERTAINTIES DUE TO INCOMPLETE b-QUARK THERMALIZATION

Since b quarks (or B mesons) are not expected to kinetically equilibrate in central collisions at RHIC (and possibly neither at LHC) [17], all previous figures included a thermal relaxation-time correction, Eq. (C7), to the equilibrium limit of Υ states in the system (Figs. 8-19). Due to the schematic character of its implementation, we study in this section how our results are affected if we make the extreme assumption of full kinetic equilibrium in the bottom sector, *i.e.*, set $\mathcal{R} \equiv 1$ (note that the rate equation (3) is applicable for both of the limiting cases, $\mathcal{R} \equiv 1$ and $\mathcal{R} \equiv 0$). We will again do this within the quasifree dissociation scenario including in-medium binding energies where the rates, and therefore the sensitivity, are largest. The results are summarized in Figs. 20 and 21. Even though the relative increase in $N_\Upsilon^{\rm eq}$ is substantial, its impact at RHIC (Fig. 20) is still rather limited (∼20%) since it becomes comparable to initial hard production (after nuclear absorption) only after $t \simeq 2$ fm/c when the temperature has dropped below 200 MeV, and consequently the reaction rates have become small, cf. Fig. 5. At LHC (Fig. 21), even though the relative increase in $N_\Upsilon^{\rm eq}$ is smaller than at RHIC (since the b-quark relaxation time is smaller at larger temperatures), its absolute number is now closer to the actual Υ number, $N_\Upsilon(t)$, in the system, especially at intermediate times in the QGP evolution ($t \simeq$ 2-4 fm/c). Since the reaction rates at this stage are still sizable, the final number in the thermal-equilibrium scenario increases by about a factor of 2 over the off-equilibrium case. Nevertheless, the main feature of a strong suppression is preserved (about a factor of 3), while the final yield is composed to about ∼90% of regenerated Υ's. This should have noticeable consequences for p_t-spectra (regenerated Υ's are expected to have much softer spectra than primordial ones, see, *e.g.*, the recent analyses in Refs. [13, 14]), and

presumably even more so for the elliptic flow (compare, *e.g.*, Refs. [58] and [13] indicating a difference of up to factor $\sim$5 in v_2 for the charmonium case).

[1] F. Karsch and E. Laermann, In Hwa, R.C. (ed.) et al.: *Quark gluon plasma* 1, and arXiv:hep-lat/0305025.
[2] T. Umeda, K. Nomura and H. Matsufuru, Eur. Phys. J. C **39S1**, 9 (2005).
[3] M. Asakawa and T. Hatsuda, Phys. Rev. Lett. **92**, 012001 (2004).
[4] S. Datta, F. Karsch, P. Petreczky and I. Wetzorke, Phys. Rev. D **69**, 094507 (2004).
[5] M. Asakawa, T. Hatsuda and Y. Nakahara, Nucl. Phys. A **715**, 863 (2003) [Nucl. Phys. Proc. Suppl. **119**, 481 (2003)].
[6] R.L. Thews, M. Schroedter and J. Rafelski, Phys. Rev. C **63**, 054905 (2001).
[7] L. Grandchamp, R. Rapp and G.E. Brown, Phys. Rev. Lett. **92**, 212301 (2004).
[8] P. Braun-Munzinger and J. Stachel, Nucl. Phys. A **690**, 119 (2001).
[9] M. I. Gorenstein, A. P. Kostyuk, L. McLerran, H. Stöcker and W. Greiner, J. Phys. G **28**, 2151 (2002).
[10] L. Grandchamp and R. Rapp, Phys. Lett. B **523**, 60 (2001).
[11] A. Andronic, P. Braun-Munzinger, K. Redlich and J. Stachel, Phys. Lett. B **571**, 36 (2003).
[12] T. Matsui and H. Satz, Phys. Lett. B **178**, 416 (1986).
[13] V. Greco, C.M. Ko and R. Rapp, Phys. Lett. B **595**, 202 (2004).
[14] R.L. Thews and M.L. Mangano, Phys. Rev. C **73**, 014904 (2006).
[15] B. Svetitsky, Phys. Rev. D **37**, 2484 (1988).
[16] M.G. Mustafa, D. Pal, D.K. Srivastava and M. Thoma, Phys. Lett. B **428**, 234 (1998).
[17] H. van Hees and R. Rapp, Phys. Rev. C **71**, 034907 (2005).
[18] H. van Hees, V. Greco and R. Rapp, Phys. Rev. C **73**, 034913 (2006).
[19] J.F. Gunion and R. Vogt, Nucl. Phys. B **492**, 301 (1997).
[20] D. Pal, B. K. Patra and D.K. Srivastava, Eur. Phys. J. C **17**, 179 (2000).
[21] V.P. Goncalves, Phys. Lett. B **518**, 79 (2001).
[22] M. E. Peskin, Nucl. Phys. B **156**, 365 (1979).
[23] G. Bhanot and M. E. Peskin, Nucl. Phys. B **156**, 391 (1979).
[24] M. Bedjidian *et al.*, arXiv:hep-ph/0311048.
[25] P. Levai, B. Muller and X. N. Wang, Phys. Rev. C **51**, 3326 (1995).
[26] S. Eidelman *et al.* [Particle Data Group], Phys. Lett. B **592**, 1 (2004).
[27] R. Vogt, Heavy Ion Phys. **18**, 11 (2003).
[28] R. Vogt [Hard Probe Collaboration], Int. J. Mod. Phys. E **12**, 211 (2003).
[29] D. Kharzeev, C. Lourenco, M. Nardi and H. Satz, Z. Phys. C **74**, 307 (1997).
[30] B. Kopeliovich, A. Tarasov and J. Hüfner, Nucl. Phys. A **696**, 669 (2001).
[31] L. Grandchamp and R. Rapp, Nucl. Phys. A **709**, 415 (2002).
[32] B.L. Combridge, Nucl. Phys. B **151**, 429 (1979).
[33] F. Karsch, M.T. Mehr and H. Satz, Z. Phys. C **37**, 617 (1988).
[34] W.M. Alberico, A. Beraudo, A. De Pace and A. Molinari, Phys. Rev. D. **72**, 114011 (2005).
[35] B. Zhang, C.M. Ko, B.A. Li, Z.W. Lin and S. Pal, Phys. Rev. C **65**, 054909 (2002).
[36] E.L. Bratkovskaya, W. Cassing and H. Stöcker, Phys. Rev. C **67**, 054905 (2003).
[37] R. Rapp and L. Grandchamp, J. Phys. G **30**, S305 (2004).
[38] R. Rapp, Phys. Rev. C **63**, 054907 (2001).
[39] P. F. Kolb and R. Rapp, Phys. Rev. C **67**, 044903 (2003).
[40] R. Rapp, J. Phys. **G31**, S217 (2005).
[41] Y. Akiba *et al.* [PHENIX Collaboration], nucl-ex/0510008.
[42] C. A. Gagliardi [STAR Collaboration], arXiv:nucl-ex/0512043.
[43] T. Affolder *et al.* [CDF Collaboration], Phys. Rev. Lett. **84**, 2094 (2000).
[44] D. Kharzeev, E. Levin and M. Nardi, Nucl. Phys. A **747**, 609 (2005)
[45] B. Alessandro *et al.* [NA50 Collaboration], Eur. Phys. J. C **39**, 335 (2005).
[46] F. Becattini, Phys. Rev. Lett. **95**, 022301 (2005).
[47] F. Karsch, E. Laermann and A. Peikert, Nucl. Phys. B **605**, 579 (2001).
[48] P. Petreczky and K. Petrov, Phys. Rev. D **70**, 054503 (2004).
[49] S. Digal, P. Petreczky and H. Satz, Phys. Rev. D **64**, 094015 (2001).
[50] C.Y. Wong, Phys. Rev. C **72**, 034906 (2005).
[51] E.V. Shuryak and I. Zahed, Phys. Rev. C **70**, 021901(R) (2004).
[52] M. Mannarelli and R. Rapp, Phys. Rev. C **72**, 064905 (2005).
[53] T. Umeda and H. Matsufuru, Nucl. Phys. Proc. Suppl. **140**, 547 (2005).
[54] F.O. Duraes, H. Kim, S.H. Lee, F.S. Navarra and M. Nielsen, Phys. Rev. C **68**, 035208 (2003).
[55] O. Kaczmarek and F. Zantow, arXiv:hep-lat/0506019.
[56] K. Petrov, Eur. Phys. J. C **43**, 67 (2005).
[57] B.B. Back *et al.* [PHOBOS Collaboration], Nucl. Phys. A **757**, 28 (2005).
[58] X.N. Wang and F. Yuan, Phys. Lett. B **540**, 62 (2002).